Why Does NGC 1068 Have a More Powerful Active Galactic Nucleus than NGC 4258 ?

Takashi Murayama and Yoshiaki Taniguchi
Astronomical Institute, Tohoku University, Aoba, Sendai 980-77
E-mail (TM): murayama@astr.tohoku.ac.jp

(Received 10 April 1997; accepted 9 May 1997)

To appear in Publications of the Astronomical Society of Japan

ABSTRACT

The nuclear gas kinematics probed by water vapor maser emission has shown that two nearby active galaxies, NGC 1068 and NGC 4258, have a supermassive object in their nuclei and their masses are nearly comparable; a few 10^7 solar masses. Nevertheless, the activity of the central engine of NGC 1068 is more powerful by two orders of magnitude than that of NGC 4258. Since it is generally considered that the huge luminosities of active galactic nuclei are attributed to the mass accretion onto a supermassive black hole, the above observational results suggest that the accretion rate in NGC 1068 is much higher than that in NGC 4258. Comparing the kinematical properties of the accreting molecular clouds between NGC 1068 and NGC 4258, we find possible evidence for dynamical gas accretion in NGC 1068, which may be responsible for the more powerful central engine in this galaxy.

Subject headings: galaxies: individual (NGC 1068 and NGC 4258) — galaxies: kinematics and dynamics — galaxies: nuclei — masers

1. Introduction

NGC 1068 is the archetypical nearby active galaxy (cf. Antonucci, Miller 1985) while NGC 4258 belongs to a class of low-ionization nuclear emission-line regions (LINER; Heckman 1980). The recent very-long-baseline interferometry (VLBI) measurements of H_2O maser emission of these two galaxies have shown that high-density molecular gas clouds are orbiting around their central, massive object (Miyoshi et al. 1995; Greenhill et al. 1995, 1996; Gallimore et al. 1996a). Although both the galaxies have a hidden active galactic nucleus (AGN) (Antonucci, Miller 1985; Wilkes et al. 1995), their observational properties are quite different. In table 1, we compare the observational properties of the central engines and the molecular gas tori in NGC 1068 and NGC 4258. The comparisons of hard X-ray, radio continuum, and Hβ luminosities between them show

that NGC 1068 is brighter intrinsically by two orders of magnitude than NGC 4258. In spite of this significant difference in luminosity of the central engines, the estimated nuclear mass of NGC 1068[1] ($M_{\rm nuc} \simeq 2.8 \times 10^7 M_\odot$) is almost comparable to that of NGC 4258 ($M_{\rm nuc} \simeq 3.6 \times 10^7 M_\odot$). It is usually considered that AGNs are powered by an accreting, supermassive black hole (Lynden-Bell 1969; Rees 1984). In this model, the bolometric luminosity of central engines depends solely on the mass accretion rate and thus there is no dependency on the central black hole mass. Therefore, the above observations suggest that the mass accretion rate in NGC 1068 is much higher than that in NGC 4258. In order to understand what happens in both the nuclei, we compare the dynamical properties of the masing molecular tori between the two galaxies and show possible evidence for dynamical accretion of molecular gas in NGC 1068.

2. Discussion

In order to consider a possible mechanism which explains why NGC 1068 has a more powerful AGN than NGC 4258, we compare the observational properties of the H_2O masing clouds between NGC 1068 and NGC 4258. In figure 1, we show the schematic illustration of the observed H_2O maser emission of NGC 1068 (Greenhill et al. 1996) and NGC 4258 (Miyoshi et al. 1995; Greenhill et al. 1995). First, we summarize the observational properties of the molecular torus in NGC 4258. The H_2O maser emission consists of the two components (Miyoshi et al. 1995; Greenhill et al. 1995): 1) One is the main component whose observed velocity corresponds to the systemic one. This emission arises near the inner edge of the torus along the line of sight. This component is due to background amplified-beamed emission. And, 2) the other is the high-velocity components which come from the two tangential sections of the molecular torus. Since there is no background continuum source for these components, it is considered that they are due to self amplification along the long gain paths[2]. The typical line width of each maser emission line, ~ 1 km s^{-1}, gives a path length of ~ 0.01 pc (Miyoshi et al. 1995). In summary, the masing emission of NGC 4258 comes from these two portions of the molecular torus. It should be mentioned that the masing emission is *not* observed from the shaded area shown in figure 1 because of either the short path length or no background continuum source (Miyoshi et al. 1995; Greenhill et al. 1995).

---

[1]The estimate of the nuclear mass of NGC 1068: The VLBI measurement of H_2O maser emission by Greenhill et al. (1996) gives the observed rotational velocity, $v_{\rm rot} \simeq 300$ km s^{-1}, at the inner radius of the sub-Keplerian ring, $r_{\rm in} = 0.56$ pc. Adopting an angle between the rotational axis of the torus and the line of sight, $\phi \simeq 40^\circ$ (Young et al. 1996), we obtain the nuclear mass, $M_{\rm nuc} \simeq 2.8 \times 10^7 M_\odot$ at distance 22 Mpc.

[2]X-ray irradiation has been considered to be important for masing of the 22 GHz transition of water vapor (Neufeld et al. 1994; Maloney et al. 1996; Wallin, Watson 1997). In terms of this mechanism, typical path lengths enough to cause the observed maser emission would be of order 0.001 pc (Wallin, Watson 1997), being shorter than that stated in Miyoshi et al. (1995). If each cloud has an diameter of 0.001 pc, the maser emission could occur in a single cloud. However, if this is the case, we could observe maser emission form the entire ring, being inconsistent with the observations. In any case, in order to explain the observed high velocity components, the argument on path length given in Miyoshi et al. (1995) and Greenhill et al. (1995) must be appreciated.

Next we discuss the H_2O maser emission of NGC1068. We should mention that the kinematical property of the maser emission of NGC 1068 is significantly different from that of NGC 4258. In NGC 4258, the high-velocity components are seen only in the portions of Keplerian ring where the path length is long enough to achieve self-amplification (Miyoshi et al. 1995; Greenhill et al. 1995). On the other hand, in the case of NGC 1068, there appear many masing clouds in the "*unseen*" area in which self amplification cannot be achieved; e.g., the component No. 4 and the majority of component No. 3 identified by Greenhill et al. (1996). In order to elucidate difference in kinematical property of the masing clouds between NGC 1068 and NGC 4258, we estimate quantitatively the unseen area of masing tori in both galaxies. Since a long path length ($\simeq$ 0.01 pc; Miyoshi et al. 1995) is necessary to cause the self-amplified masing in a molecular torus with the (sub-) Keplerian rotation, most parts of the molecular ring become to be the unseen area (Miyoshi et al. 1995; Greenhill et al. 1995). We consider a molecular torus with a radial velocity distribution of $v_{\rm c}(r) = v_{\rm in}\ (r/r_{\rm in})^a$ where $v_{\rm c}(r)$ is the circular velocity at radius r and $v_{\rm in}$ is the circular velocity at the inner edge of the torus ($r_{\rm in}$) [see figure 1]. The power index, a, is -0.5 for the Keplerian torus (i.e., for NGC 4258) while -0.31 for NGC 1068 (Greenhill et al. 1996). The velocity gradient along the line of sight is given by the derivative,

$$\frac{dv_{\rm l}(r)}{dy} = \frac{1}{2}\ (a-1)\ \omega_{\rm c}(r)\ \sin 2\theta \qquad (1)$$

where $v_{\rm l}(r) = v_{\rm c}(r)\sin\theta$ is the line of sight velocity at radius r and $\omega_{\rm c}(r) = v_{\rm c}(r)/r$. The definition of θ is shown in figure 1. In the unseen area, the velocity change (Δv) within a path length (l) should be larger than 1 km s^{-1} (Miyoshi et al. 1995); i.e., $|dv_{\rm l}(r)/dy| > \Delta v/l$. This condition gives a constraint on the unseen angle, θ,

$$\sin 2\theta\ >\ \frac{2\Delta v/l}{|a-1|\ \omega_{\rm c}(r)}. \qquad (2)$$

In the lower panel of figure 1, we show the unseen area for both NGC 4258 and NGC 1068. Here we adopt $(v_{\rm in}, r_{\rm in})$ = (1080 km s^{-1}, 0.13 pc) for NGC 4258 and $(v_{\rm in}, r_{\rm in})$ = (300 km s^{-1}, 0.56 pc) for NGC 1068. In the case of NGC 4258, it is shown that the high velocity component can arise from the tangential sections of the torus, being consistent with the observations (Miyoshi et al. 1995; Greenhill et al. 1995). As for the main component, if we assume the point-like continuum radiation source, we need an opening angle of 7° (Miyoshi et al. 1995). Since, however, this angle is larger than the critical unseen angle (0°.5), we consider that the continuum source may have a spatial extent of $\sim$ 0.01 pc (cf. Haschick, Baan 1994). Although the unseen area estimated for the case of NGC 1068 is basically similar to that of NGC 4258, the observed appearance of the masing clouds in NGC 1068 is significantly different from that of NGC 4258. Therefore, we must consider some other different masing mechanisms for the masing clouds of NGC 1068 which appear in the unseen area.

Greenhill et al. (1996) proposed that the maser emission comes from the limb of the torus

rather than the midplane. Though they argued that the orbital motion is parallel to the line of sight along the limb and produces a substantial amplification. However, since the limb may co-rotate with the midplane (i.e., the sub-Keplerian rotation), it is unlikely that only the gas clouds on the limb can gain the long path. Therefore, the masing regions cannot be attributed to the sub-Keplerian rotating molecular torus. It is thus suggested that they come from dense molecular clouds inside the torus[3]. In order for such clouds to gain the long path length, the velocity structure should obey a rigid-body rotation. There are two alternatives for such a cloud system. One is a gaseous bar (or an oval ring) with a figure rotation. Since the sub-Keplerian torus suggests the presence of gravitational disturbance to this torus, it is likely that there is the inner non-axisymmetric potential like a bar structure. The other possibility is that clumpy molecular clouds rotate like a rigid body as a whole. A typical size of each cloud would be as large as ~ 0.01 pc to gain the long path length enough to cause the masing. However, each cloud itself may rotate because of the conservation of angular momentum. Thus if this is the case, each cloud would rotate as a rigid body rotator again.

Here a key question arise as how to make such a gaseous bar or a clumpy cloud system inside the torus. The gradual accumulation of gas clouds toward the central region of the galaxy causes over density in the gas cloud system. Once the gas mass exceeds about one tenth of the dynamical mass within the concerned region, the gas may experience the gravitational instability because of its self gravity, leading to the formation of either a bar (Shlosman et al. 1989; Shlosman et al. 1990; Wada, Habe 1995) or clumpy gas clouds (Shlosman, Noguchi 1993; Heller, Shlosman 1994). If the gas mass within $r \simeq 0.56$ pc would exceed $\sim 3 \times 10^6 M_\odot (\sim 0.1 \times M_{\rm nuc})$, the gravitational instability may occur in the nuclear gas of NGC 1068. Although, however, NGC 1068 has abundant dense gas in the nuclear region (Tacconi et al. 1994), the gas mass associated with the dusty torus is estimated to be $\sim 3 \times 10^4 M_\odot$ at most (Pier, Krolik 1992b, 1993). It is therefore unlikely that the rigid-body component comes from the gravitational instability of the torus itself. Taking the more powerful central engine of NGC 1068 into account, we may consider that the inner radius of the torus in NGC 1068 would be once much smaller. If this is the case, we expect that the inner parts of the molecular torus may be broken by the intense radiation field (cf. Pier, Krolik 1992a; see also Neufeld, Maloney 1995). Although we cannot specify the actual geometry of the rigid-body component, we show our modest interpretation schematically in figure 2.

Finally we estimate a possible gas accretion rate from the inner torus broken by the intense radiation in NGC 1068. Since it is considered that the gas clouds broken by the radiation may accrete in a characteristic time which is roughly comparable to the free fall time there, $t_{\rm ff} = \sqrt{r^3/(GM_{\rm nuc})} \sim 10^3$ years for $r = 0.5$ pc. Since, however, we do not take the angular momentum loss into account in this estimate, this timescale should be considered as a lower limit. The gas mass broken by the radiation may be the same order as that of the present torus,

[3]Begelman, Bland-Hawthorn (1997) reported that the masing clouds in the nuclear region of NGC 1068 are distributed in the warped disk.

$M_{\rm cloud} \sim 10^4 M_\odot$, giving a nominal *dynamical* accretion rate as $\dot{M}_{\rm acc}({\rm Dyn}) \sim M_{\rm cloud}/t_{\rm ff} \leq 10 M_\odot$ y^{-1}. Though it is hard to estimate the effect of angular momentum loss accurately because of ambiguity in the physical and dynamical condition of the nuclear gas, we may estimate the probable accretion timescale from the actual size of the narrow line region (NLR) in NGC 1068. Given the size of the NLR, $r_{\rm NLR} \simeq 900$ pc at the distance $D = 22$ Mpc (Schmitt, Kinney 1996), the timescale (i.e., the lifetime of the central engine) is estimated to be $t_{\rm acc} \sim r_{\rm NLR}/(\beta c) \sim 3 \times 10^4/(\beta/0.1)$ years where βc is the net velocity of the ionizing radiation (c is the light velocity in the vacuum). Here we assume $\beta \sim 0.1$ because it is unlikely that the ionizing radiation is highly relativistic (cf. Gallimore et al. 1996b). Since this timescale is more reliable than that estimated above, we obtain the most probable dynamical accretion rate, $\dot{M}_{\rm acc}({\rm Dyn}) \sim 0.3(\beta/0.1) M_\odot$ y^{-1}. Next, we estimate another accretion rate based on the bolometric luminosity. Pier et al. (1994) gave the bolometric luminosity of the central engine in NGC 1068, $L_{\rm bol} \simeq 8.5 \times 10^{44}$ $(f_{\rm refl}/0.01)^{-1}(D/22{\rm Mpc})^2$ erg s^{-1} where $f_{\rm refl}$ is the fraction of nuclear flux reflected into our line of sight and D is the distance to NGC 1068. Adopting the fiducial values in Pier et al. (1994), we obtain the gas accretion rate based on the luminosity, $\dot{M}_{\rm acc}({\rm Lum}) = L_{\rm bol}/(\eta_{\rm acc} c^2) \simeq 0.02$ $(L_{\rm bol}/10^{44}$ erg s$^{-1})(\eta_{\rm acc}/0.1)^{-1} \simeq 0.17$ $M_\odot$ y^{-1} where $\eta_{\rm acc}$ is the conversion efficiency from the gravitational energy to the radiation. Since this value is almost consistent with the dynamical one, we consider that the dynamical accretion may be responsible for the activity in NGC 1068.

In conclusion, the striking difference of the molecular gas tori between NGC 1068 and NGC 4258 is the presence/absence of a rigid-body rotating component which may be formed through the destruction of the innermost torus by the strong radiation from the central engine. This component may provide direct evidence for dynamical accretion of the nuclear gas in NGC 1068. Since this component is not observed in the less-luminous AGN of NGC 4258, we suggest that this component is responsible for the more powerful AGN in NGC 1068.

We would like to thank Lincoln Greenhill and Naomasa Nakai for helpful discussion about the H_2O maser in NGC 1068 and NGC 4258. We also thank Kazuo Makishima for useful comments of the X-ray property of NGC 4258 and the referee, Jun Fukue, for kind comments which improved this paper. This work was supported by the Ministry of Education, Science, Sports, and Culture (No. 07044054). TM was supported by the Grant-in-Aid for JSPS Fellows by the Ministry of Education, Science, Sports, and Culture.

REFERENCES

Antonucci, R. R. J., Miller, J. S. 1985, ApJ 297, 621

Begelman, M. C., Bland-Hawthorn, J. 1997, Nature 385, 22

Gallimore, J. F., Baum, S. A., O'Dea, C. P. 1996b, ApJ 464, 198

Gallimore, J. F., Baum, S. A., O'Dea, C. P., Brinks, E., Pedlar, A. 1996a, ApJ 462, 740

Greenhill, L. J., Gwinn, C. R., Antonucci, R., Barvanis, R. 1996, ApJ 472, L21

Greenhill, L. J., Jiang, D. R., Moran, J. M., Reid, M. J., Lo, K. Y., Claussen, M. J. 1995, ApJ 440 619

Heckman, T. M. 1980, A&A 87, 141

Haschick, A. D., Baan, W. A., Peng, E. W. 1994, ApJ 437, L35

Heller, C. H., Shlosman, I. 1994, ApJ 424, 84

Hummel, E., Krause, M., Lesch, H. 1989, A&A 211, 266

Koyama, K., Inoue, H., Tanaka, Y., Awaki, H., Takano, S., Ohashi, T., Matsuoka, M. 1989, PASJ 41, 731

Lynden-Bell, D. 1969, Nature 223, 690

Maloney, P. P., Hollenbach, D. J., Tielens, G. G. M. 1996, ApJ 466, 561

Marshall, F. E., Netzer, H., Arnaud, K. A., Boldt, E. A., Holt, S. S., Jahoda, K. M., Kelley, R., Mushotzky, R. F. et al. 1993, ApJ 405, 168

Makishima, K., Fujimoto, R., Ishisaki, I., Kii, T., Loewenstein, M., Mushotzky R., Serlemitsos, P., Sonobe, T. et al. 1994, PASJ 46, L77

Miller, J. S., Goodrich, R. W. 1990, ApJ 355, 456

Miyoshi, M., Moran, J., Herrnstein, J., Greenhill, L., Nakai, N., Diamond, P., Inoue, M. 1995, Nature 373, 127

Nakai, N., Inoue, M., Miyazawa, K., Miyoshi, M., Hall, P. 1995, PASJ 47, 771

Neufeld, D. A., Maloney, P. P. 1995, ApJ 447, L17

Neufeld, D. A., Maloney, P. P., Conger, S. 1994, ApJ 436, L127

Pier, E. A., Krolik, J. H. 1992a, ApJ 399, L23

Pier, E. A., Krolik, J. H. 1992b, ApJ 401, 99

Pier, E. A., Krolik, J. H. 1993, ApJ 418, 673

Pier, E. A., Antonucci, R., Hunt, T., Kriss, G., Krolik, J. 1994, ApJ 428, 124

Rees, M. J. 1984, ARA&A 22, 471

Shlosman, I., Frank, J., Begelman, M. C. 1989, Nature 338, 45

Shlosman, I., Begelman, M. C., Frank, J. 1990, Nature 345, 679

Shlosman, I., Noguchi, M. 1993, ApJ 414, 474

Schmitt, H. R., Kinney, A. L. 1996, ApJ, 463, 498

Tacconi, L. J., Genzel, R., Blietz, M., Cameron, M., Harris, A. I., Madden, S. 1994, ApJ 426, L77

Ulvestad, J. S., Wilson, A. S. 1984, ApJ 285, 439

Wada, K., Habe, A. 1995, MNRAS 277, 433

Wallin, B. K., Watson, W. D. 1997, ApJ 476, 685

Wilkes, B. J., Schmidt, G. D., Smith, P. S., Mathur, S., McLeod, K. K. 1995, ApJ 455, L13

Young, S., Packham, C., Hough, J. H., Efstathiou, A. 1996, MNRAS 283, L1

Table 1. Comparison of NGC 1068 and NGC 4258.

	Unit	NGC 1068	NGC 4258
Distance	Mpc	22 (1)	6.4 (2)
Central mass ($M_{\rm nuc}$)	$M_\odot$	2.8×10^7 (3)	3.6×10^7 (2)
Hβ luminosity† ($L_{\rm H\beta}$)	erg s^{-1}	2.0×10^{42} (4)	1.4×10^{40} (5)
X-ray luminosity†† ($L_{\rm X}$)	erg s^{-1}	10^{43-44} (6)	3.3×10^{40} (7)
20 cm radio power ($P_{\rm 20cm}$)	W Hz^{-1}	2.2×10^{23} (8)	4.0×10^{21} (9)
H_2O maser luminosity ($L_{\rm H_2O}$)	$L_\odot$	145 (10)	125 (10)
	Molecular torus		
Inner radius ($r_{\rm in}$)	pc	0.56 (11)	0.13 (2)
Outer radius ($r_{\rm out}$)	pc	1.0 (11)	0.25 (2)
Inner rotation velocity ($v_{\rm in}$)	km s^{-1}	300 (11)	1080 (2)
Inclination	degree	$\sim 40 \pm 5$ (12)	83 ± 4 (2)
Position angle	degree	~ 45 (11)	86 ± 2 (2)

† The intrinsic luminosity of the hidden, broad Hβ emission; $L_{\rm H\beta} = L^{\rm p}_{\rm H\beta}(\Delta\Omega/4\pi)^{-1}\ \tau^{-1}P^{-1}$ where $L^{\rm p}_{\rm H\beta}$ is the polarized Hβ luminosity, $\Delta\Omega$ is the covering factor in steradian, τ is the scattering optical depth, and P is the fractional polarization (Miller, Goodrich 1990). We adopt ($\tau\Delta\Omega/4\pi$, P) = (0.034, 0.16) for NGC 1068 and (0.034, 0.094) for NGC 4258. Here we assume that NGC 4258 has the same value of $\tau\Delta\Omega/4\pi$ as that of NGC 1068. The intrinsic Hβ luminosity is considered to be proportional to the bolometric luminosity.

†† The reddening-corrected hard X-ray luminosity (2 - 10 keV).

Refs.: 1) This value is usually adopted, corresponding to the recession velocity 1,100 km s^{-1} with a Hubble constant $H_0 = 50$ km s^{-1} Mpc^{-1}. 2) Miyoshi et al. (1995). 3) This paper (see the footnote). 4) Miller and Goodrich (1990). 5) Wilkes et al. (1995). 6) Koyama et al. (1989). 7) Makishima et al. (1994). 8) Ulvestad and Wilson (1984), 9) Hummel et al. (1989). 10) Nakai et al. (1995). 11) Greenhill et al. (1996). And, 12) Young et al. (1996). Note that this value is obtained not for the molecular torus but for the dusty one.

Figure Captions

Fig. 1: The unseen area of masing tori for NGC 4258 and NGC 1068.

Fig. 2: Schematic comparison of the molecular tori of NGC 1068 (Greenhill et al. 1996) and NGC 4258 (Miyoshi et al. 1995; Greenhill et al. 1995) probed by the H_2O maser emission. Although the rotation of the actual molecular torus of NGC 4258 is clockwise, we adopt the counterclockwise rotation for both types nominally.

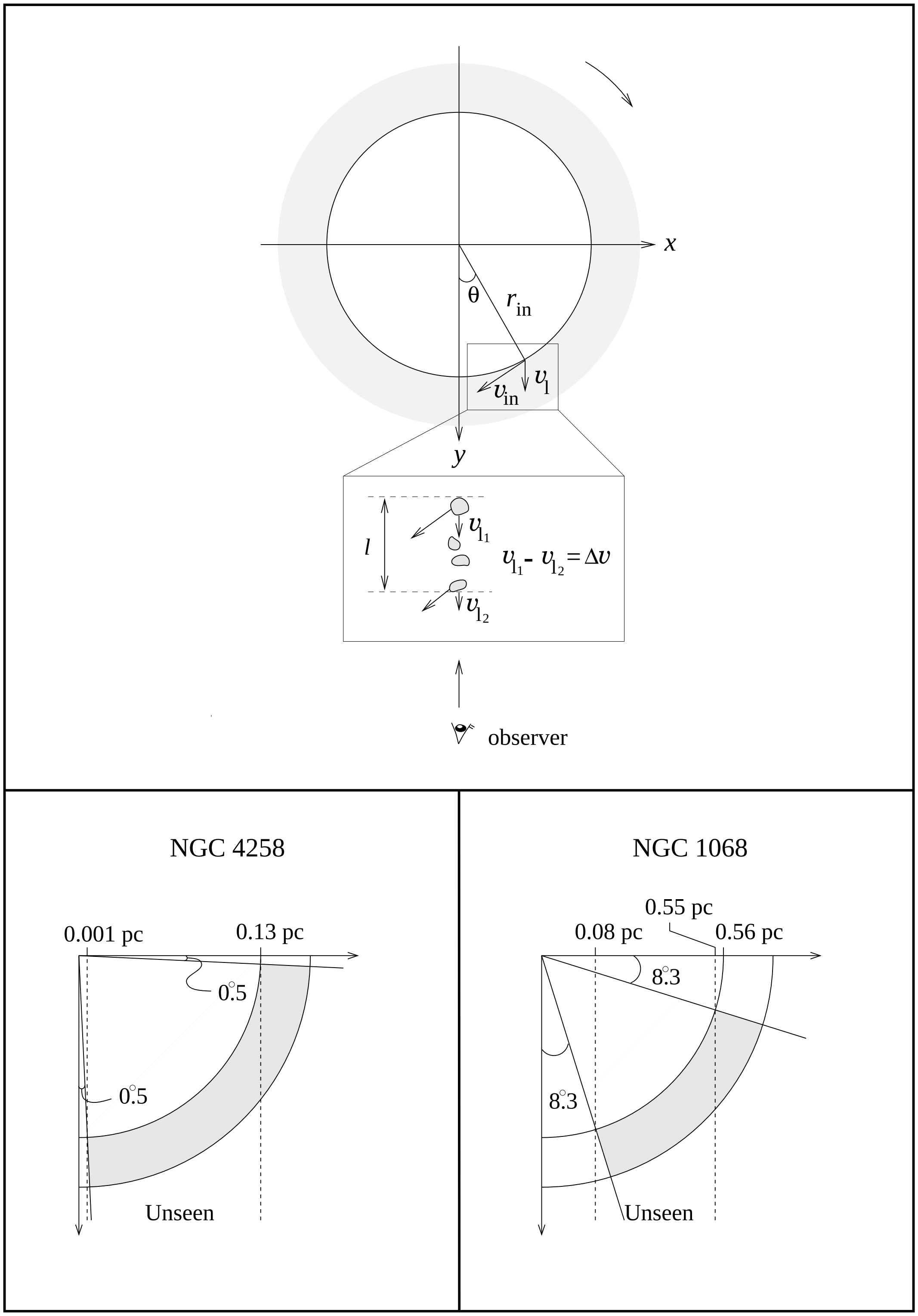
x
θ
r_{in}
v_{in}
v_l
y
l
v_{l_1}
$v_{l_1} - v_{l_2} = \Delta v$
v_{l_2}
observer
NGC 4258
0.001 pc
0.13 pc
0.°5
0.°5
Unseen
NGC 1068
0.55 pc
0.08 pc
0.56 pc
8.°3
8.°3
Unseen

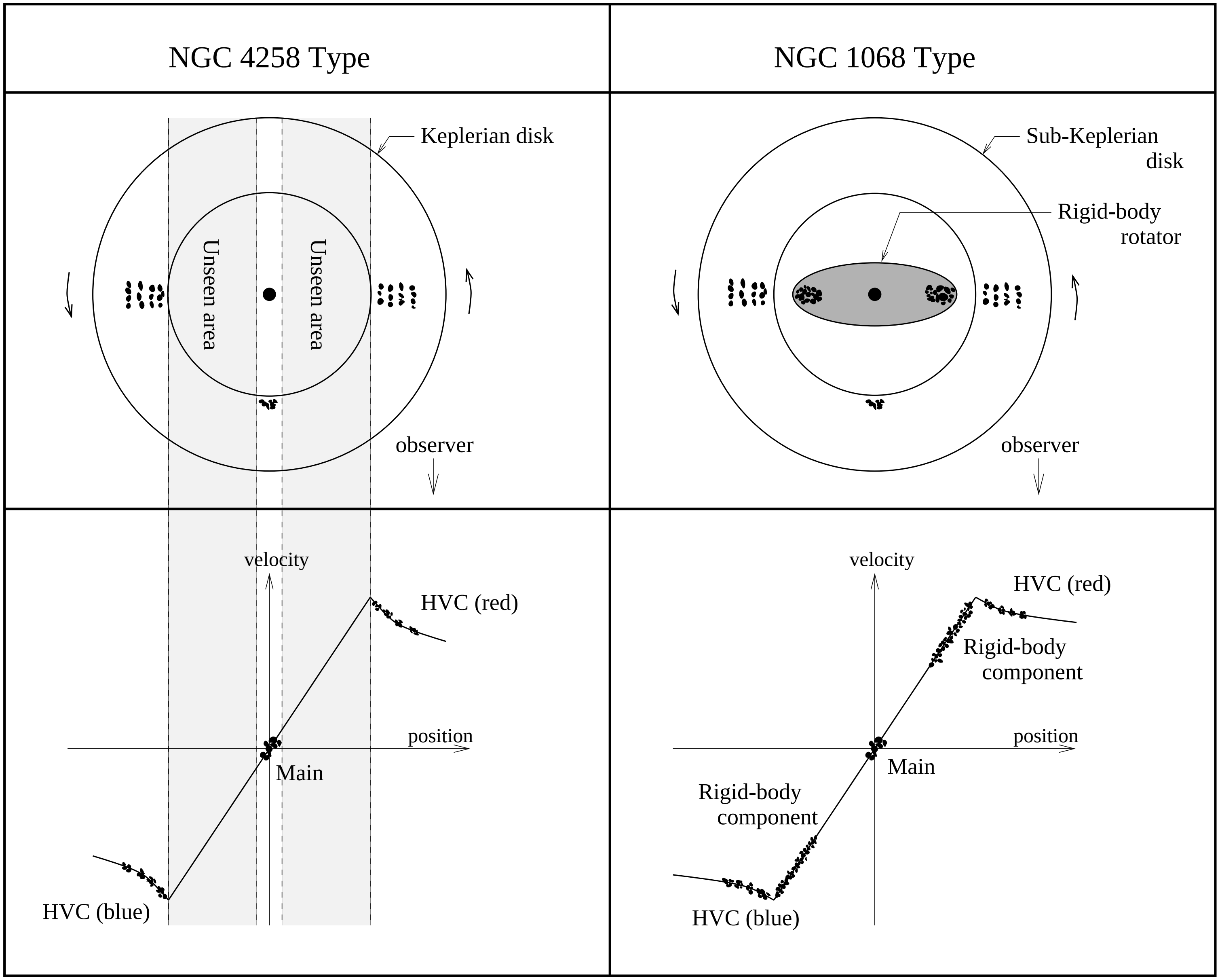
NGC 4258 Type
NGC 1068 Type
Keplerian disk
Unseen area
Unseen area
observer
Sub-Keplerian disk
Rigid-body rotator
observer
velocity
HVC (red)
position
Main
HVC (blue)
velocity
HVC (red)
Rigid-body component
position
Main
Rigid-body component
HVC (blue)